Calculations of Molecular Properties in Hybrid Coupled-Cluster and Molecular Mechanics Approach

J. R. Hammond,[†,‡] **M. Valiev,***[,‡] **W. A. deJong,**[‡] **and K. Kowalski***[,‡]

Department of Chemistry and the James Franck Institute, The University of Chicago, Chicago, Illinois 60637, and William R. Wiley Environmental Molecular Sciences Laboratory, Battelle, Pacific Northwest National Laboratory, K8-91, P.O. Box 999, Richland, Washington 99352

Received: January 22, 2007; In Final Form: April 12, 2007

We report benchmark calculations obtained with our new coupled-cluster singles and doubles (CCSD) code for calculating the first- and second-order molecular properties. This code can be easily incorporated into combined [Valiev, M.; Kowalski, K. *J. Chem. Phys.* **2006**, *125*, 211101] classical molecular mechanics (MM) and ab initio coupled-cluster (CC) calculations using NWChem, enabling us to study molecular properties in a realistic environment. To test this methodology, we discuss the results of calculations of dipole moments and static polarizabilities for the Cl_2O system in the CCl_4 solution using the CCSD (CC with singles and doubles) linear response approach. We also discuss the application of the asymptotic extrapolation scheme (AES) [Kowalski, K.; Valiev, M. *J. Phys. Chem. A* **2006**, *110*, 13106] in reducing the numerical cost of CCSD calculations.

1. Introduction

The coupled-cluster methodology[1−9] has become one of the most widely used tools in quantum chemistry. Over the last two decades numerous variants and extensions were designed not only to treat the energetics of ground and excited states but also to calculate the molecular properties. In contrast to the finite field approaches based on the numerical differentiation of the electronic energy over external field strength, the CC linear response theory (CC-LR)[10,11] enables us to obtain expressions for static and/or frequency dependent properties in a compact analytical manner. Different levels of CC theory corresponding to increasing excitation ranks of cluster operators were tested for first-, second-, third-, and higher-order properties. Among them, the linear response CC with singles and doubles (CCSD-LR)[12] and with singles, doubles, and triples (CCSDT-LR)[13] approaches providing different levels of description of correlation effects now have a chance to be used in realistic calculations. To save the big numerical overhead associated with full inclusion of triply excited clusters, several iterative methods such as CCSDT-*n* ($n = 1-3$)[14,15] and CC3[16] have been tested, leading to consistent improvements with respect to the CCSD-LR results. Recently, Kállay and co-workers have implemented general order CC[17] including energy derivatives[18] and response functions.[19]

In realistic simulations of molecules in solution, electron correlation effects and the effect of the surrounding environment are equally important. For this purpose, one frequently combines the ab initio methodology (QM) with classical molecular mechanics (MM). The QM/MM approach[20] was recently extended by Christiansen and co-workers to include linear response functions for coupled-cluster (CC) wavefunctions,[21] and applied to electric moments[22] and to excited states and polarizabilities[23] of liquid water.

Recently, two of the authors developed an efficient multiscale dynamical framework for high-level calculations of finite temperature ground and excited-state properties.[24] We illustrated the performance of this approach on the excited states of cytosine base in the native DNA environment using a variant of completely renormalized equation of motion coupled-cluster formalism with singles, doubles and noniterative triples (CR-EOMCCSD(T))[42] method to describe the quantum region. For obvious reasons the integration of the CCSD property codes with the QM/MM module is also important. Therefore, in this paper, we discuss preliminary results for the dipole moments and static polarizabilities obtained with combined linear response CCSD and MM approaches. As a benchmark system for the CCSD/MM simulation we use the Cl_2O molecule in the CCl_4 solution (Figure 1).

Another problem that may heavily impact future QM/MM simulations of molecular properties is the ability of reducing the overall time required by multiple calls to rather expensive ab initio procedures for quantum region. In a long-term perspective, the numerical demands of the CC-like approaches can hamper the widespread use of the CC techniques in the context of QM/MM simulations. Several techniques based on the Laplace or Cholesky decomposition[25−28] of perturbative denominators, methods striving at the reduction of the virtual orbital space,[29,30] or localized approaches[31−34] are very promising in this matter. Also another class of approaches based on the extrapolation schemes such as correlation energy extrapolation by intrinsic scaling (CEEIS),[35−38] or extrapolation approaches for second-order energies developed by Ayala, Scuseria, and Savin[39] (for rigorous bounds for extrapolated correlation energies see ref 40), seem to be very effective in attaining good estimates of correlation energies.

We have recently proposed an approximate scheme based on the asymptotic extrapolation scheme,[41] which allowed us to extrapolate the excitation energies as a function of simple cutoff factor for orbitals energies of correlated unoccupied orbitals for fraction of time required by full calculations. We clearly

---

[*] To whom correspondence should be addressed. E-mail: K.K., karol.kowalski@pnl.gov; M.V., marat.valiev@pnl.gov.

[†] The University of Chicago.

[‡] Pacific Northwest National Laboratory.

10.1021/jp070553x CCC: \$37.00

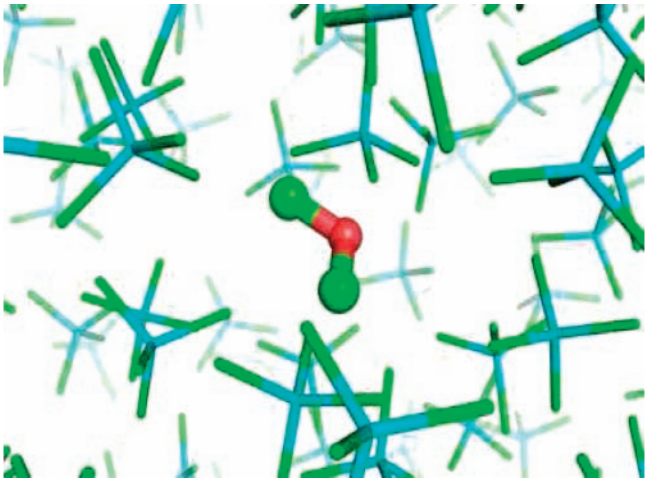

Figure 1. Schematic representation of the Cl_2O molecule in CCl_4 solution. B3LYP optimized geometries in POL1 basis set are: $R_{O-Cl} = 1.73$ Å and $\alpha_{Cl-O-Cl} = 112.47°$). All core orbitals were kept frozen.

demonstrated that for the valence excited states the loss of accuracy was on the order of few hundreds of electronvolts. We believe that similar arguments can be used in the CC property calculations. However, before going to large scale QM/MM simulations we want to estimate the effectiveness of the AES using simple gas-phase systems.

The organization of this papers is as follows: in section 2 we give a brief description of the most basic features of linear response theory and asymptotic extrapolation scheme. In section 3 we discuss the results of our simulations for Cl_2O molecule in the gas-phase and CCl_4 solution.

2. Theory

This section describes two main threads in our methodology development. The first thread concerns the seamless integration of the CC-based property calculations and the other deals with the possible application of the recently developed asymptotic extrapolation scheme in the calculations of molecular properties. Because the CC and its linear response extension has been described in a number of papers,[10,11] in this section we present only salient features of this methodology (for details see Kallay and Gauss[19]). We also give a short description of the QM/MM interface we used in our calculations and AES-related issues.

2.1. Coupled-Cluster Energy Functional. The coupled-cluster wavefunction is described by

$$|\Psi_{CC}\rangle = \exp(T)|\Phi\rangle \tag{1}$$

where $|\Psi\rangle$ denotes the reference functions, usually chosen as Hartree−Fock determinant, and the cluster operator, T, is given by

$$T = T_1 + T_2 + ... + T_M \tag{2}$$

$$T_m = \frac{1}{(m!)^2} \sum_{i_1,...,i_m} \sum_{a_1,...,a_m} t^{a_1...a_m}_{i_1...i_m} X^{\dagger}_{a_1} ... X^{\dagger}_{a_m} X_{i_m} ... X_{i_1} \tag{3}$$

where $X^{\dagger}_p$ (X_p) are the creation (annihilation) operators. As always, the i, j, k, ... (a, b, c, ...) indices refer to occupied (unoccupied) spin−orbitals in the reference $|\Phi\rangle$. For the exact theory the M parameter corresponds to the total number of correlated electrons (N), whereas all approximate formalisms use $M \ll N$. In this paper we focus our attention on the CC method with singles and doubles (CCSD),[43] i.e., $M = 2$. The quantities $t^{a_1...a_m}_{i_1...i_m}$ are referred to as the cluster amplitudes.

The standard coupled-cluster energy expression is obtained by projecting the standard energy eigenvalue relationship onto $\langle 0|\exp(-T)$,

$$E_{CC} = \langle \Phi|\exp(-T)H\exp(T)|\Phi\rangle \tag{4}$$

The coupled-cluster similarity-transformed Hamiltonian, $\bar{H} = \exp(-T)H\exp(T)$, will be used to simplify subsequent equations. Projection of the $\bar{H}$ onto m-fold ($m = 1$, ..., M) excitation manifolds produces the coupled-cluster equations

$$0 = \langle \Phi^{a_1...a_m}_{i_1...i_m}|\bar{H}|\Phi\rangle \tag{5}$$

$$|\Phi^{a_1...a_m}_{i_1...i_m}\rangle = X^{\dagger}_{a_1}...X^{\dagger}_{am} X_{i_m}...X_{i_1}|\Phi\rangle \tag{6}$$

where the order of the excitation manifold equals the order of the cluster operator, T_m, to obtain a soluble set of linear equations.

2.2. First Derivatives of the Energy. Molecular property calculations require energy derivatives, which can be symbolically represented by dE/dx, where x is a parameter that defines the electronic Hamiltonian $H(x)$ (for simplicity, we will denote this Hamiltonian by H). For example, x can correspond to the nuclear geometries of the system or the strength of the external electric field. Straightforward differentiation of the coupled-cluster energy functional in eq 4,

$$\frac{dE_{CC}}{dx} = \left\langle 0\middle|\exp(-T)\frac{\partial H}{\partial x}\exp(T)\middle|0\right\rangle + \left\langle 0\middle|\exp(-T)\left[H,\frac{\partial T}{\partial x}\right]\exp(T)\middle|0\right\rangle \tag{7}$$

requires amplitude derivatives for every perturbation parameter, x. However, by introducing Lagrange multipliers,[44] which eliminate the need of calculating of the cluster operator derivatives ($\partial T/\partial x$), we obtain a new energy functional that satisfies the generalized Hellmann−Feynman theorem[45] and is valid for all energy derivatives,

$$\tilde{E}_{CC} = \langle \Phi|(1 + \Lambda)\bar{H}|\Phi\rangle \tag{8}$$

where

$$\Lambda = \Lambda_1 + \Lambda_2 + ... + \Lambda_M \tag{9}$$

$$\Lambda_m = \frac{1}{(m!)^2} \sum_{i_1,...,i_m} \sum_{a_1,...,a_m} \lambda^{i_1...i_m}_{a_1...a_m} X^{\dagger}_{i_1} ... X^{\dagger}_{i_m} X_{a_m} ... X_{a_1} \tag{10}$$

The Lagrange multipliers are obtained by projection onto n -fold excitation manifolds on the right

$$0 = \langle \Phi|(1 + \Lambda)\bar{H}|\Phi^{a_1...a_m}_{i_1...i_m}\rangle \tag{11}$$

The first derivatives of the energy with respect to any parameter can now be written

$$\frac{dE_{CC}}{dx} = \left\langle \Phi\middle|(1 + \Lambda)\exp(-T)\frac{\partial H}{\partial x}\exp(T)\middle|\Phi\right\rangle \tag{12}$$

2.3. Second Derivatives of the Energy. Second derivatives of the coupled-cluster energy functional can be obtained from the original energy formula (eq 4),

$$\frac{\mathrm{d}^2E_{\mathrm{CC}}}{\mathrm{d}x\,\mathrm{d}y} = \left\langle\Phi\left|\exp(-T)\frac{\partial^2 H}{\partial x\partial y}\exp(T)\right|\Phi\right\rangle + \hat{P}(x,y)\left\langle\Phi\left|\exp(-T)\left[\frac{\partial H}{\partial y},\frac{\partial T}{\partial x}\right]\exp(T)\right|\Phi\right\rangle + \left\langle\Phi\left|\exp(-T)\left[H,\frac{\partial^2 T}{\partial x\partial y}\right]\exp(T)\right|\Phi\right\rangle + \left\langle\Phi\left|\exp(-T)\left[\left[H,\frac{\partial T}{\partial y}\right],\frac{\partial T}{\partial x}\right]\exp(T)\right|\Phi\right\rangle \quad (13)$$

where $\hat{P}(x,y)\,f(x,y) = f(x,y) + f(y,x)$. This formula uses amplitude second derivatives and requires the solution of $|\{x\}||\{y\}|$ additional sets of linear equations. Alternatively, second derivatives can be obtained from the coupled-cluster lambda energy functional (eq 8) using the symmetric formulation,

$$\frac{\mathrm{d}^2\tilde{E}_{\mathrm{CC}}}{\mathrm{d}x\,\mathrm{d}y} = \left\langle 0\left|(1+\Lambda)\exp(-T)\frac{\partial^2 H}{\partial x\partial y}\exp(T)\right|0\right\rangle + \hat{P}(x,y)\left\langle 0\left|(1+\Lambda)\exp(-T)\left[\frac{\partial H}{\partial y},\frac{\partial T}{\partial x}\right]\exp(T)\right|0\right\rangle + \left\langle 0\left|(1+\Lambda)\exp(-T)\left[\left[\frac{\partial H}{\partial y},\frac{\partial T}{\partial y}\right],\frac{\partial T}{\partial x}\right]\exp(T)\right|0\right\rangle \quad (14)$$

or the asymmetric formulation,

$$\frac{\mathrm{d}^2\tilde{E}_{\mathrm{CC}}}{\mathrm{d}x\,\mathrm{d}y} = \left\langle 0\left|(1+\Lambda)\exp(-T)\frac{\partial^2 H}{\partial x\partial y}\exp(T)\right|0\right\rangle + \left\langle 0\left|(1+\Lambda)\exp(-T)\left[\frac{\partial H}{\partial x},\frac{\partial T}{\partial y}\right]\exp(T)\right|0\right\rangle + \left\langle 0\left|\frac{\partial \Lambda}{\partial y}\exp(-T)\frac{\partial H}{\partial x}\exp(T)\right|0\right\rangle \quad (15)$$

which require the solution of $|\{x\} \cap \{y\}|$ or $2\cdot|\{y\}|$ additional sets of linear equations, respectively. The optimal choice between these two depends on the type of perturbation x and y correspond to.

2.4. Coupled-Cluster Linear Response. Once the Hamiltonian $H(\lambda)$ can be represented in a simple form $H(\lambda) = H_0 + \lambda O$, where H_0 is the original electronic Hamiltonian for isolated system, λ is a scalar, and operator O is considered as a perturbation (in our case, O is the dipole operator to model the effect of an weak external electric field), then the derivatives of energy and cluster operator can be easily related to the coefficients in the perturbative expansion for the energy and cluster operator,

$$E(\lambda) = E^{(0)} + \lambda E^{(1)} + \lambda^2 E^{(2)} + ... \quad (16)$$

$$T(\lambda) = T^{(0)} + \lambda T^{(1)} + \lambda^2 T^{(2)} + ... \quad (17)$$

Straightforward algebra leads to

$$E^{(1)} = \langle\Phi|\exp(-T)\,O\exp(T)|\Phi\rangle + \langle\Phi|\exp(-T)[H,T^{(1)}]\exp(T)|\Phi\rangle \quad (18)$$

and the connection to eq 7 is obvious. The projected response equations to be solved are

$$0 = \langle\Phi^{a_1...a_m}_{i_1...i_m}|\exp(-T)\,O\exp(T)|\Phi\rangle + \langle\Phi^{a_1...a_m}_{i_1...i_m}|\exp(-T)\,[H,T^{(1)}]\exp(T)|\Phi\rangle \quad (19)$$

which can be written as $A\mathbf{x} + \mathbf{b} = 0$, with x corresponding to the perturbed amplitudes, as stated by Monkhorst.[10] From $T^{(0)}$, $\Lambda^{(0)}$, and $T^{(1)}$, we calculate the second-order response energy using eq 14, where $T^{(1)} = \partial T/\partial x$. The asymmetric formulation of the coupled-cluster linear response was implemented for CCSD in the NWChem[46] software suite using the Tensor Contraction Engine.[49−51]

2.5. Asymptotic Extrapolation Scheme. The time requirements of CC calculations can be significantly reduced by using asymptotic extrapolation schemes introduced in the context of excited-state calculations and described in ref 41. We start from noticing that the whole set of correlated spin−orbitals (Ω) can be decomposed into two subsets

$$\Omega = \Omega_\tau + \bar{\Omega}_\tau \quad (20)$$

where the Ω_τ and $\bar{\Omega}_\tau$ sets are composed of all correlated occupied spin−orbitals and correlated virtual orbitals with corresponding orbital energies below the value of the τ factor and all virtual orbitals with orbitals energies being greater than the τ parameter, respectively. This decomposition induces decomposition of the algebra of operators expressed in the second quantized formalism. Each of these operators X, representing for example the Hamiltonian or cluster operators, can be decomposed as follows:

$$X = X_\tau + \bar{X}_\tau \quad (21)$$

where X_τ represents part of the X operator expressed in terms of spin−orbital indices from the set Ω_τ and each term in $\bar{X}_\tau$ contains at least one index from $\bar{\Omega}_\tau$. This leads to the following form of CC equations:

$$Q_\tau[(H_\tau \mathrm{e}^{T_\tau})_{\mathrm{C}} + (\bar{H}_\tau \mathrm{e}^{T_\tau+\bar{T}_\tau})_{\mathrm{C}}]|\Phi\rangle = 0 \quad (22)$$

$$\bar{Q}_\tau[(H_\tau \mathrm{e}^{\bar{T}_\tau})_{\mathrm{C}} + (\bar{H}_\tau \mathrm{e}^{T_\tau+\bar{T}_\tau})_{\mathrm{C}}]|\Phi\rangle = 0 \quad (23)$$

where Q_τ and $\bar{Q}_\tau$ are projection operators on the manifold of excited configurations used to define components T_τ and $\bar{T}_\tau$ ($T = T_\tau + \bar{T}_\tau$), respectively. The $\bar{H}_\tau$ operator in eqs 22 and 23 should not be confused with the similarity-transformed Hamiltonian. Using current notation, the $\bar{H}_\tau$ operator refers to the part of second quantized electronic Hamiltonian that contains at least one spin−orbital index from $\bar{\Omega}_\tau$. Although both sets of equations labeled by Q_τ and $\bar{Q}_\tau$ projections are coupled with respect to amplitudes defining the T_τ and $\bar{T}_\tau$ components, for sufficiently large values of the τ parameter we can anticipate that the most important correlation effects are already included in the T_τ part. This enables us to approximate the $\bar{Q}_\tau$ equations by $((H_\tau + \bar{H}_\tau)\bar{T}_\tau)_{\mathrm{C}} + (\bar{H}_\tau \mathrm{e}^{T_\tau})_{\mathrm{C}}$. For example, the approximate formula for doubly excited $\bar{T}_\tau$ amplitudes then becomes

$$\bar{t}^{ij}_{ab} \simeq \frac{1}{\epsilon_i + \epsilon_j - \epsilon_a - \epsilon_b}\langle\Phi^{ab}_{ij}|(\bar{H}_\tau \mathrm{e}^{T_\tau})_{\mathrm{C}}|\Phi\rangle \quad (24)$$

Because the orbital energy differences in eq 24 are on the order of τ ($\epsilon_i + \epsilon_j - \epsilon_a - \epsilon_b = O(\tau)$) the $\bar{T}_\tau$ amplitudes reveal an $1/\tau$ behavior in the asymptotic limit. This simple observation can be easily generalized to Λ and/or $T^{(1)}$ operators ($\Lambda = \Lambda_\tau + \bar{\Lambda}_\tau$, $T^{(1)} = T^{(1)}_\tau + \bar{T}^{(1)}_\tau$), although the $T^{(1)}$ case requires special attention because the operators (such as the dipole moment), having no obvious interpretation in the language of energy differences, are involved in the equations for $T^{(1)}$.

In analogy to the asymptotic schemes used to extrapolate the excitation energies, the same reasoning can be employed in calculating properties. For example, using the bivariational approach,[47] the expectation value for any one-body operator can be written as

$$\langle\rho\rangle = \langle\Phi|(1 + \Lambda_\tau + \bar{\Lambda}_\tau)(\mathrm{e}^{-(T_\tau+\bar{T}_\tau)}(\rho_\tau + \bar{\rho}_\tau)\mathrm{e}^{T_\tau+\bar{T}_\tau})|\Phi\rangle \quad (25)$$

Grouping all terms depending on Ω_τ-label creation/annihilation operators (i.e., the Λ_τ, ρ_τ, and T_τ operators) we can rewrite $\langle\rho\rangle$ as

$$\langle\rho\rangle = \langle\rho_\tau\rangle + \bar{\nu}_\tau \quad (26)$$

where $\langle\rho_\tau\rangle = \langle\Phi|(1 + \Lambda_\tau)(\mathrm{e}^{-T_\tau}\rho_\tau\mathrm{e}^{T_\tau})|\Phi\rangle$ and $\bar{\nu}_\tau$ decays at least as $1/\tau$ in the asymptotic limit. It is convenient to exploit formula (26) to extrapolate to the exact value obtained for a given level of theory using the full set of correlated spin−orbitals. We will use simple functions such as $f(\tau) = a_1 + \sum_{i=1,n} a_{i+1}/\tau^{i+1}$ to find the best fit to several values of $\langle\rho_\tau\rangle$ obtained in calculations for various values of τ.

An important issue concerns the size-consistency of the AES results. In the general case, the AES does not have to be rigorously size-consistent, even though the extrapolation is based on the sample points that correctly dissociate in the noninteracting subsystem limit. Another reason for this can be attributed to the τ-dependence of the basic operators. In calculations for a given τ value the T_τ and $T_\tau^{(1)}$ operators do not have to lead to size-consistent results even though they are obtained from explicitly connected equations (the equations for Λ_τ include some disconnected but linked terms, which in calculating the properties, when the HF reference is employed, are fully contracted to connected operators such as $\mathrm{e}^{-T_\tau}\rho_\tau\mathrm{e}^{T_\tau}$ leading to connected property diagrams). To arrive at the size consistency of approximate CC approaches, one has to be able to separately localize the set of occupied and unoccupied orbitals in the noninteracting subsystems limit (for exhaustive discussion of related issues see ref 48). Because approaches such as the CCSD, CCSDT, etc. are invariant under the rotations of occupied and unoccupied orbitals this localization does not have to be done explicitly. However, by cutting off all virtual orbitals above some τ threshold we may define virtual Ω_τ space, which in noninteracting subsystems limit cannot be localized. The control of localization properties for all Ω_τ spaces used by AES can be hard to achieve for larger systems. In such cases the rigorous size-consistency may be only approximately restored in the extrapolation process.

3. Computational Details

The NWChem[46] computational chemistry software was used to perform the calculations. All linear response codes as well as the second quantized expressions for static polarizabilities were automatically generated by TCE.[49−51] Calculations for the Λ_{CCSD} operator and the CCSD dipole moments were performed using code implemented by Hirata.[49] In all codes a new and more efficient way of handling two-electron integrals and related offset-tables was used.[52]

In the gas-phase calculations for the Cl_2O molecule we used Sadlej's (POL1)[54] and aug-cc-pVXZ (X = D,T,Q) basis sets.[55] In all calculations all core electrons were kept frozen and Cartesian representation of the angular-momentum functions was used for the POL1 and aug-cc-pVXZ (X = D,T,Q) basis sets. We optimized ground-state geometry with the B3LYP and CCSD(T) approaches using the aug-cc-pVTZ basis set. As seen from Table 1, the equilibrium value of $R_{\mathrm{O-Cl}}$ is nearly the same for both approaches discussed in the Table 1. The more substantial differences occur for the Cl−O−Cl angle. Although the CCSD(T) method predicts its value to be 110.849°, the B3LYP value is significantly different and equals 112.603°. Because the first- and second-order properties may be sensitive to such geometry changes we decided to use the CCSD(T) equilibrium geometry in all gas-phase calculations presented here (see Tables 2 and 3).

TABLE 1: Optimized Ground-State Energies and Geometries Obtained with the B3LYP and CCSD(T) Approaches Using the aug-cc-pVTZ Basis Set[a]

method	total energy	$R_{\mathrm{O-Cl}}$	$\alpha_{\mathrm{Cl-O-Cl}}$
B3LYP	−995.598665	1.71437	112.60327
CCSD(T)	−994.486282	1.71399	110.84889

[a] Cartesian representation of d functions was used in calculations.

TABLE 2: CCSD Dipole Moments and Polarizabilities Obtained for the Cl_2O Molecule for the LR-CCSD(T),IB Equilibrium Geometry (Table 1)[a]

basis set	α_{XX}	α_{YY}	α_{ZZ}	$\Delta\alpha$	$\bar{\alpha}$	μ
POL1	53.711	29.167	32.102	23.216	38.327	−0.228
aug-cc-pVDZ	52.364	27.002	30.233	23.911	36.533	−0.223
aug-cc-pVTZ	53.272	28.300	31.479	23.544	37.962	−0.237
aug-cc-pVQZ	53.457	28.646	31.783	23.401	37.462	−0.237

[a] All core orbitals were kept frozen.

The description of the effect of the environment on the molecular system is an extremely difficult task. Usually, this is achieved within a combined QM/MM formalism, which requires inclusion of the correlation effects for the quantum region as well as description of interaction between QM and MM parts. The QM/MM formalism has been implemented using CC theory by Christiansen and co-workers[23,56−58] including linear response functions, and by two of the authors[24] including a temperature dependent formalism for calculating excitation energies. The QM/MM Hamiltonian used in this work,

$$H = H_{\mathrm{QM}} + H_{\mathrm{QM/MM}} + H_{\mathrm{MM}} \quad (27)$$

is optimized including static charges, but the complete linear response function of Christiansen and co-workers[21] has not been used because the QM charge density response is not included (column four in Table 1 of ref 23). In the absence of this term, a simple way to increase the accuracy of this approach is to include the first solvation shell within the QM part of the calculation. Although this is computationally expensive, it is likely to be as accurate, if not more so, than treating the first solvation shell using polarizable force fields with more terms in the response function.

Our system was composed of a Cl_2O embedded in a cubic box in 215 CCl_4 molecules. The quantum region consisted of the Cl_2O molecule with the rest of the system treated at the molecular mechanics level using Amber force field parameters.[59] After the initial QM/MM DFT optimization of the entire system the solvent (CCl_4) was brought to equilibrium over the course of 3.8 ns QM/MM molecular dynamics simulation at constant temperature and pressure (298.15 K, 1.025×10^5 Pa) with a 15 Å cutoff. During this dynamical run the QM region was represented by a set of fixed effective charges. These were updated approximately every 0.5 ns by means of QM/MM electrostatic potential fitting using DFT/B3LYP level of theory and POL1 basis set.[54] After the solvent equilibration, the entire system was optimized once more using multiregion QM/MM optimization at the DFT/B3LYP level of theory. This gave rise to a final structure for the QM/MM coupled-cluster property calculations. Two types of calculations were performed to asses

TABLE 3: Extrapolated Values of the CCSD Polarizabilities and Dipole Moment of the Cl_2O Molecule Obtained with Asymptotic Extrapolation Scheme (AES)[a]

property	$\tau_1 = 1.5$	$\tau_2 = 2.0$	$\tau_3 = 2.5$	$\tau_4 = 3.0$	$\tau_5 = 3.5$	$\tau_6 = 4.0$	$f_1^{(A)}$	$f_1^{(B)}$	$f_2^{(A)}$	$f_2^{(B)}$	full CCSD
α_{XX}	53.979	54.046	53.932	54.016	53.977	53.972	53.920	53.970	54.252	53.873	53.457
α_{YY}	29.675	29.725	29.458	29.361	29.318	29.317	28.856	29.052	29.752	28.603	28.646
α_{ZZ}	32.540	32.611	32.472	32.413	32.401	32.383	32.149	32.286	32.573	31.941	31.783
μ	−0.174	−0.183	−0.184	−0.207	−0.206	−0.205	−0.236	−0.228	−0.232	−0.251	−0.237

[a] Two functions were used in extrapolation $f_1(\tau) = x_1 + x_2/\tau$ and $f_2(\tau) = x_1 + x_2/\tau + x_3/\tau^2$. Versions A and B refer to five-point $\{\tau_2, \tau_3, \tau_4, \tau_5, \tau_6\}$ and six-point $\{\tau_1, \tau_2, \tau_3, \tau_4, \tau_5, \tau_6\}$ extrapolation schemes, respectively. The aug-cc-pVQZ basis set was used (Cartesian representation of d functions was employed) and all core orbitals were kept frozen. The energy of the highest molecular orbital is equal to 226.088907 hartree.

the influence of the solvent. The first one ignored the presence of solvent altogether (gas phase), and the second included all the solvent charges on the system (a total of 1075) using the same geometry structure of the Cl_2O molecule.

4. Results and Conclusions

This section is divided into two parts: the first part deals with the effectiveness of AES in calculating molecular properties in the gas-phase using various basis sets, the second part reports the results of our combined CC/MM formalism. Because the Cl_2O has recently attracted a considerable amount of attention and was a subject of experimental studies in the CCl_4 solution[53] we think it is worthwhile to use our combined CC/MM formalism to model the experimental conditions and estimate the effect of the surrounding environment on the dipole moments and static polarizabilities of Cl_2O molecule.

Table 2 summarizes our calculations for dipole moments, static polarizabilities, polarizability anisotropy ($\Delta\alpha$), and average polarizability ($\bar{\alpha}$). One can notice that the POL1 results, which were specially designed for molecular properties, are very close to the results obtained with the aug-cc-pVQZ basis set, although the aug-cc-pVQZ basis set is almost 3 times bigger than the POL1 basis set. For example, the absolute values of discrepancies between POL1 and aug-cc-pVQZ basis set results amount to 0.254, 0.521, and 0.319 au for α_{XX}, α_{YY}, and α_{ZZ}, respectively. The agreement between predicted dipole values is much better. The POL1 and aug-cc-pVQZ differ by only 0.009 au. At the same time the differences between the aug-cc-pVDZ (the dimension of the aug-cc-pVDZ basis set (83) is roughly the same as the dimension of the POL1 basis set (94)) are much larger. The 1.644 au of difference for α_{YY} calculated in aug-cc-pVDZ and aug-cc-pVQZ once again emphasizes the efficiency of the POL1 basis set in describing molecular properties.

The efficiency of the AES can be easily evaluated by analyzing Table 3 that summarizes different extrapolation schemes. At the very core of the AES lies the reduction of the overall numerical cost by using possibly small values of the τ parameter. At the same time chosen τ values (or sample points) should be big enough to guarantee the proper asymptotic behavior of the τ-dependent properties. Sometimes the simultaneous fulfillment of these two conflicting needs may be quite a challenging task. In our studies we used the following values of τ: $\tau_1 = 1.5$, $\tau_2 = 2.0$, $\tau_3 = 2.5$, $\tau_4 = 3.0$, $\tau = 3.5$, and $\tau = 4.0$. For each point the overall cost of the CCSD properties calculations is significantly reduced compared to the full CCSD counterpart. To be more specific, for $\tau_1 = 1.5$ only 87 virtual orbitals are correlated, which results in about 140-fold speed-up of the CCSD calculations (total number of virtual orbitals is equal to 298), whereas for $\tau_6 = 4.0$, 158 virtual orbitals are used in calculations resulting in almost 13-fold speed-up of the CCSD part. Also the choice of the trial function used for extrapolation plays a critical role. We used two, probably the most rudimentary forms of the trail functions: $f_1(\tau) = x_1 + x_2/\tau$ and $f_2(\tau) = x_1 + x_2/\tau + x_3/\tau^2$ that reflect the asymptotic, $1/\tau$ behavior of the τ-expansion. To explore the impact of low values of τ parameter, we decided to employ two sets of τ points. The first set (A) is composed of $[\tau_2, \tau_3, \tau_4, \tau_5, \tau_6]$ and the second set (B) contains all six τ values, i.e., $[\tau_1, \tau_2, \tau_3, \tau_4, \tau_5, \tau_6]$ including τ_1. These choices of the sample points are also consistent with our general observation that, contrary to the valence excited states case,[41] to get reliable results for molecular properties, one has to apply the AES to the sequence of single point calculations corresponding to larger values of the τ parameter. These poorer convergence properties of the AES may be a consequence of the fact that the observables involved in property calculations, such as dipole moments are not directly related to the energy differences, which in turn may lead to slower convergence of corresponding $1/\tau$-expansion.

The results of the $f_1(\tau)$ and $f_2(\tau)$ extrapolations based on (A) and (B) sets of sample points (defining the $f_1(\tau)^{(A)}$, $f_1(\tau)^{(B)}$, $f_2(\tau)^{(A)}$, $f_2(\tau)^{(B)}$ schemes) are collected in Table 3. Of all approaches shown in this table, the performance of the $f_2(\tau)^{(B)}$ seems to be the most accurate regarding the achieved accuracies for the polarizabilities. For example, the $f_2(\tau)^{(B)}$ absolute errors with respect to the full CCSD results amount to 0.416, 0.043, and 0.158 au for α_{XX}, α_{YY}, and α_{ZZ}, respectively. By going from the $f_2(\tau)^{(B)}$ scheme to the $f_2(\tau)^{(A)}$ one can clearly demonstrate the importance of the sampling of small τ values in situations when the maximum value of the τ parameter (in our case this is the $\tau_6 = 4.0$ point) still provides significant reduction of the full CCSD cost. The $f_2(\tau)^{(A)}$ errors are considerably bigger than the $f_2(\tau)^{(B)}$ ones and equal 0.795, 1.106, and 0.790 au for α_{XX}, α_{YY}, and α_{ZZ}, respectively. None of the $f_1(\tau)$ schemes can compete with the $f_2(\tau)^{(B)}$ version regarding accuracies for static polarizabilities. The situation is slightly different for dipole moment, which seems to be the best described by the $f_1(\tau)^{(A)}$, $f_1(\tau)^{(B)}$ variants despite of the irregular behavior of the CCSD dipole moment as a function of the τ parameter. The corresponding errors with respect to the full CCSD calculations are 0.001 and 0.009 au, respectively. Although the polarizability values vary monotonically for $\tau \geq 3.0$ (which may be the first indication of working in the $(1/\tau)$ regime for polarizabilities), the same is not true for dipole moments that reveal oscillatory behavior in the $[\tau_3, \tau_4, \tau_5]$ interval. For this reason larger values of τ need to be used to get a more reliable picture. Yet another issue concerns level of theory employed. In the excited-state calculations, the EOMCCSD excitation energies supplemented with the noniterative corrections due to triples were the subject of the extrapolation procedures, but in the present studies all quantities of interest were obtained on the singles and doubles level. Summarizing this part of the discussion, one should conclude that it is possible to obtain reliable AES results for molecular properties provided that the set of sample points is correctly defined until undesired oscillatory behavior of a given property is eliminated.

TABLE 4: CCSD Polarizabilities (α_{XX}, α_{YY}, α_{ZZ}), Average Polarizabilities ($\bar{\alpha}$), and Polarizability Anisotropy ($\Delta\alpha$) Obtained for the Solution and the Gas Phase Using the POL1 Basis Set.[54,a]

	α_{XX}	α_{YY}	α_{ZZ}	$\bar{\alpha}$	$\Delta\alpha$
gas phase (gas struct)	55.705	29.314	32.371	39.130	25.003
gas phase (sol. struct)	55.631	29.309	32.357	39.099	24.939
solution	55.497	29.247	32.351	39.065	24.785
Δ (gas struct)	0.208	0.067	0.020	0.065	0.218
Δ (sol. struct)	0.134	0.062	0.006	0.034	0.154

[a] In all calculations all core electrons were kept frozen and Cartesian representation of d orbitals was employed (see text for details). Δ rows are defined in terms of geometry relaxation (difference between the gas-phase and solution-phase structure without an environment) and solvent interaction (difference between a molecule in the gas phase and in solution).

As seen from Table 4, the effect of the environment is estimated to be rather small, which is not unexpected, as CCl_4 is a nonpolar solvent. The most prone to external perturbation seems to be the α_{XX} component of the polarizability tensor (for simplicity we brought the polarizability tensor to diagonal form). Though the corresponding influence of solvation on α_{XX} amounts to 0.208 au, the remaining differences for α_{YY} and α_{ZZ} are significantly smaller, with values of 0.067 and 0.020 au, respectively. For $\bar{\alpha}$ and $\Delta\alpha$ the shifts are on the order of 0.07 and 0.22 au. It is also interesting to analyze the results in terms of contributions due to geometry relaxation of the Cl_2O molecule in the CCl_4 solution and those due to the presence of the charge density of the CCl_4 solution around the molecule. One can immediately see that the largest contribution comes from the inclusion of the CCl_4 charge density. For example, the geometry relaxation effect for the α_{XX} component of the polarizability tensor is 0.074 au, whereas the effect due to the presence of the solvent molecules is 0.134 au. Because the correlation effects for the ground state are rather mild, we do not expect triply excited clusters to change these values significantly.

Acknowledgment. This work has been performed using the Molecular Science Computing Facility (MSCF) in the William R. Wiley Environmental Molecular Sciences Laboratory (EMSL) at the Pacific Northwest National Laboratory. The William R. Wiley Environmental Molecular Sciences Laboratory at the Pacific Northwest National Laboratory is funded by the Office of Biological and Environmental Research in the U.S. Department of Energy. The Pacific Northwest National Laboratory is operated for the U.S. Department of Energy by the Battelle Memorial Institute under Contract DE-AC06-76RLO-1830. J.R.H. is supported by the DOE-CSGF program provided under grant number DE-FG02-97ER25308. Support to M.V. from the Office of Naval Research (NOOO1406IP20027) is gratefully acknowledged.

References and Notes

(1) Coester, F. *Nucl. Phys.* **1958**, *7*, 421.

(2) Coester, F.; Kümmel, H. *Nucl. Phys.* **1960**, *17*, 477.

(3) Čižek, J. *J. Chem. Phys.* **1966**, *45*, 4256. Čižek, J.; Paldus, J. *Int. J. Quantum Chem.* **1971**, *5*, 359.

(4) Paldus, J.; Čižek, J.; Shavitt, I. *Phys. Rev. A* **1972**, *5*, 50.

(5) Paldus, J. In *New Horizons of Quantum Chemistry*; Löwdin, P.-O., Pullman, B., Eds.; Reidel: Dordrecht, The Netherlands, 1983; pp 31−60. Bartlett, R. J.; Dykstra, C. E.; Paldus, J. In *Advanced Theories and Computational Approaches to the Electronic Structure of Molecules*; Dykstra, C. E., Ed.; Reidel: Dordrecht, The Netherlands, 1984; pp 127−159.

(6) Bartlett, R. J. In *Modern Electronic Structure Theory*; Yarkony, D. R., Eds.; World Scientific: Singapore, 1995; Vol. 1, pp 1047−1131.

(7) Paldus, J.; Li, X. *Adv. Chem. Phys.* **1999**, *110*, 1.

(8) Crawford, T. D.; Schaefer, H. F., IIII. *Rev. Comput. Chem.* **2000**, *14*, 33.

(9) Bartlett, R. J. In *Theory and Applications of Computational Chemistry: The First Forty Years*; Dykstra, C. E., Frenking, G., Kim, K. S., Scuseria, G. E., Eds.; Elsevier: Amsterdam, 2005; pp 1191−1221.

(10) Monkhorst, H. J. *Int. J. Quantum Chem.* **1977**, *S11*, 421. Dalgaard, E.; Monkhorst, H. J. *Phys. Rev. A* **1983**, *28*, 1217.

(11) Koch, H.; Jørgensen, P. *J. Chem. Phys.* **1990**, *93*, 3333. Christiansen, O.; Hättig, C.; Jørgensen, P. *Int. J. Quantum Chem.* **1998**, *68*, 1.

(12) Kobayashi, R.; Koch, H.; Jørgensen, P. *Chem. Phys. Lett.* **1994**, *249*, 30. Hättig, C.; Christiansen, O.; Koch H.; Jørgensen, P. *Chem. Phys. Lett.* **1997**, *269*, 428. Hättig, C.; Christiansen, O.; Jørgensen, P. *Chem. Phys. Lett.* **1998**, *282*, 139.

(13) Larsen, H.; Olsen, J.; Hättig, C.; Jørgensen, P.; Christiansen, O.; Jürgen G. *J. Chem. Phys.* **1999**, *111*, 1917.

(14) Lee, Y. S.; Bartlett, R. J. *J. Chem. Phys.* **1984**, *80*, 4371. Lee, Y. S.; Kucharski, S. A. *J. Chem. Phys.* **1984**, *81*, 5906.

(15) Noga, J.; Bartlett, R. J.; Urban, M. *Chem. Phys. Lett.* **1987**, *134*, 126.

(16) Christiansen, O.; Koch, H.; Jørgensen, P. *J. Chem. Phys.* **1995** *103*, 7429. Koch, H.; Christiansen, O.; Jørgensen, P.; Sanchez de Merás, A. M.; Helgaker, T. *J. Chem. Phys.* **1997**, *106*, 1808. Hald, K.; Pawłwski, F.; Jørgensen, P. Hättig, C. *J. Chem. Phys.* **2003**, *118* 1292.

(17) Kállay M.; Surján, P. R. *J. Chem. Phys.* **2001**, *115*, 2945.

(18) Kállay, M.; Gauss, J.; P. Szalay, G. *J. Chem. Phys.* **2003**, *119*, 2991. Kállay, M.; Gauss, J. *J. Chem. Phys.* **2004**, *120*, 6841. Kállay, M.; Gauss, J.; Szalay, P. G. *J. Chem. Phys.* **2004**, *121*, 9257.

(19) Kállay, M.; Gauss, J. *J. Mol. Struct. (THEOCHEM)* **2006**, *768*, 71.

(20) Noell J.; Morokuma, K. *Chem. Phys. Lett.* **1975**, *36*, 465. Warshel, A.; Levit, M. *J. Mol. Biol.* **1976**, *103*, 227. Singh U. C.; Kollman, P. A. *J. Comp. Chem.* **1986**, *7*, 718. Field, M. J.; Bash, P. A.; Karplus, M. *J. Comput. Chem.* **1990**, *11*, 700. Thompson, M. A. *J. Phys. Chem.* **1996**, *100*, 14492.

(21) Kongsted, J.; Osted, A.; Mikkelsen, K. V.; Christiansen, O. *Mol. Phys.* **2002**, *100*, 1813.

(22) Kongsted, J.; Osted, A.; Mikkelsen, K. V.; Christiansen, O. *Chem. Phys. Lett.* **2002**, *364*, 379.

(23) Kongsted, J.; Osted, A.; Mikkelsen, K. V.; Christiansen, O. *J. Chem. Phys.* **2003**, *118*, 1620.

(24) Valiev, M.; Kowalski, K. *J. Chem. Phys.* **2006**, *125*, 211101.

(25) Kowalski, K.; Piecuch, P. *J. Chem. Phys.* **2004**, *120*, 1715.

(26) Almlöf, J. *Chem. Phys. Lett.* **1991**, *181*, 319.

(27) Constans, P.; Ayala, P. Y.; Scuseria, G. E. *J. Chem. Phys.* **2000**, *113*, 10451.

(28) Koch, H.; Sánches de Merás, A. *J. Chem. Phys.* **2000**, *113*, 508.

(29) Koch, H.; Sánches de Merás, A.; Pedersen, T. B. *J. Chem. Phys.* **2003**, *118*, 9481.

(30) Adamowicz, L.; Bartlett, R. J. *J. Chem. Phys.* **1987**, *86*, 6314.

(31) Adamowicz, L.; Bartlett, R. J.; Sadlej, A. J. *J. Chem. Phys.* **1988**, *88*, 5749.

(32) Schütz, M.; Werner, H.-J. *Chem. Phys. Lett.* **2000**, *318*, 370.

(33) Schütz, M. *J. Chem. Phys.* **2000**, *113*, 9986.

(34) Schütz, M. *J. Chem. Phys.* **2002**, *116*, 8772.

(35) Flocke N.; Bartlett, R. J. *J. Chem. Phys.* **2004**, *121*, 10935.

(36) Bytautas L.; Ruedenberg, K. *J. Chem. Phys.* **2004**, *121*, 10905.

(37) Bytautas L.; Ruedenberg, K. *J. Chem. Phys.* **2004**, *121*, 10919.

(38) Bytautas, L.; Ruedenberg, K. *J. Chem. Phys.* **2004**, *121*, 10852.

(39) Bytautas, L.; Ruedenberg, K. *J. Chem. Phys.* **2005**, *122*, 154110.

(40) Ayala, P. Y.; Scuseria, G. E.; Savin, A. *Int. J. Quantum Chem.* **1999**, *307*, 227.

(41) Iyengar, S.; Scuseria, G. E.; Savin, A. *Int. J. Quantum Chem.* **2000**, *79*, 222.

(42) Kowalski, K.; Valiev, M. *J. Phys. Chem. A* **2006**, *110*, 13106.

(43) Purvis, G. D., III; Bartlett, R. J. *J. Chem. Phys.* **1982**, *76*, 1910.

(44) Salter, E. A.; Trucks G. W.; Bartlett, R. J. *J. Chem. Phys.* **1989**, *90*, 1752.

(45) Löwdin, P. *J. Mol. Spectrosc.* **1964**, *13*, 326.

(46) Apra, E.; Windus, T. L.; Straatsma, T. P.; Bylaska, E. J.; de Jong, W.; Kowalski, K.; Hirata, S.; Valiev, M.; Wang, D.; Hackler, M. T.; Zhao, Y.; Harrison, R. J.; Dupuis, M.; Smith, D. M. A.; Nieplocha, J.; Tipparaju, V.; Krishnan, M.; Auer, A. A.; Brown, E.; Cisneros, G.; Fann, G. I.; Fruchtl, H.; Garza, J.; Hirao, K.; Kendall, R.; Nichols, J. A.; Tsemekhman, K.; Wolinski, K.; Anchell, J.; Bernholdt, D.; Borowski, P.; Clark, T.; Clerc, D.; Dachsel, H.; Deegan, M.; Dyall, K.; Elwood, D.; Glendening, E.; Gutowski, M.; Hess, A.; Jaffe, J.; Johnson, B.; Ju, J.; Kobayashi, R.; Kutteh, R.; Lin, Z.; Littlefield, R.; Long, X.; Meng, B.; Nakajima, T.; Niu, S.; Pollack, L.; Rosing, M.; Sandrone, G.; Stave, M.; Taylor, H.; Thomas, G.; van Lenthe, J.; Wong, A.; Zhang, Z. *NWChem, A Computational Chemistry Package for Parallel Computers, Version 5.0*; Pacific Northwest National Laboratory, Richland, WA 99352-0999; 2006.

(47) Arponen, J. S. *Ann. Phys.* **1983**, *151*, 311.

(48) Jankowski, K.; Kowalski, K. *J. Chem. Phys.* **1999**, *111*, 2940.

(49) Hirata, S. *J. Phys. Chem. A* **2003**, *107*, 9887.

(50) Hirata, S. *J. Chem. Phys.* **2004**, *121*, 51.

(51) Hirata, S. *Theor. Chem. Acc.* **2006**, *116*, 2.

(52) Kowalski, K.; de Jong, W. A. Manuscript in preparation.

(53) Esposito, A. P.; Reid, P. J.; Rousslang, K. W. *J. Photochem. Photobiol.* **1999**, *129*, 9.

(54) Sadlej, A. J. *Collect. Czech. Chem. Commun.* **1988**, *53*, 1995.

(55) Dunning, T. H., Jr. *J. Chem. Phys.* **1989**, *90*, 1007. Woon, D. E.; Dunning, T. H., Jr. *J. Chem. Phys.* **1993**, *98*, 1358.

(56) Kongsted, J.; Osted, A.; Mikkelsen, K. V.; Åstrand, P.-O.; Christiansen, O. *J. Chem. Phys.* **2004**, *121*, 8435.

(57) Aidas, K.; Kongsted, J.; Osted, A.; Mikkelsen, K. V.; Christiansen, O. *J. Phys. Chem. A* **2005**, *109*, 8001.

(58) Osted, A.; Kongsted, J.; Mikkelsen, K. V.; Åstrand, P.-O.; Christiansen, O. *J. Chem. Phys.* **2006**, *124*, 124503.

(59) Fox, T.; Kollman, P. A. *J. Phys. Chem. B* **1998**, *102*, 8070.